Journal of ELECTRICAL ENGINEERING, VOL. 60, NO. 6, 2009, 313–320

GRID CONNECTED HYBRID DISPERSED POWER GENERATORS BASED ON PV ARRAY AND WIND–DRIVEN INDUCTION GENERATOR

Meenakshisundaram Arutchelvi * — **Samuel Arul Daniel** **

A grid connected hybrid scheme for residential power supply based on an integrated photo-voltaic (PV) array and a wind-driven induction generator has been proposed in this paper. This new grid-connected configuration employs a closed loop controller at the inverter interfaced to the PV array to regulate the current fed to the grid. By varying the reference current to the controller the PV array meets the reactive power needs of the induction generator (IG) and also acts as a source of real power to the grid. A dynamic mathematical model of the hybrid scheme with variables expressed in $d-q$ synchronous reference frame has been developed. The model is implemented in the Simpower^{TM} platform, the simulation results bring out the usefulness of hybrid operation of PV, and wind-driven IG for grid connected operations.

K e y w o r d s: dispersed hybrid generators, current control, voltage source inverter, wind-driven induction generator, PV array

1 INTRODUCTION

The unbundling of the conventional electric power system in a liberalized and globalized environment had resulted in more and more private agencies setting up generators which are integrated to the distribution network. Further, as stated by [1], these distributed generators are also becoming attractive due to statutes enacted for ecological and environmental protection. In this context, domestic customers are also encouraged to put up modest power plants to meet their energy requirements [2]. These distributed resources integrated to the utility grid also contribute to peak shaving and maximum demand reduction. Further, they also serve as emergency and stand-by power supply [3]. Furthermore, strides made in distribution automation, increased emphasis on reliable supply of power to sensitive loads and development of new power generation technologies had resulted in more and more number of distributed resources being commissioned nowadays. It has been pointed out by [4] that one of the imperatives in the connection of distributed resources is the requirement to satisfy the load requirement of a consumer group even when there is a failure of grid. Hence, this paper investigates one such scheme of distributed generators, where more than one renewable source is employed, so as to supply a selective load and feed the excess power to the utility and also to supply the load in the event of a grid failure.

As a matter of fact, induction generators (IG) driven by wind-turbines have been extensively employed for feeding real power to the grid [5]. Evidently, wind-driven induction generators consume reactive power and the inductive VARs required by this generator has to be supplied by the grid. However, it is well known that for an induction generator to act as an independent dispersed power generator, capacitors are required to excite the generator [6]. The transient behavior of a wind-driven induction generator when disconnected from the grid with such capacitors at the stator terminals of the machine requires careful study, since domestic customers are involved. These isolated generators also exhibit unsatisfactory voltage regulation and frequency variation. To overcome these limitations, instead of providing reactive power using a three-phase capacitor bank, inverter assisted induction generators were proposed. [7] proposed IG schemes with PWM inverters, where the excess energy was sent to the utility grid to maintain the stator voltage and frequency constant or a speed governor to control the amount of the generated energy was employed. However, these schemes are unsuitable for wind-driven isolated operations. A PWM-VSI scheme with a battery bank or a dc charged capacitor has been proposed in [8]. In this scheme, there is a possibility of a voltage collapse in the event of the battery or the capacitor being deeply discharged due to persistent low wind speeds during a particular period of the year.

Hybrid wind-solar grid integrated schemes employing wind-driven PM alternator and PV resources were attempted earlier [9]. In these schemes, the PV array output and the rectifier output fed from wind-driven permanent magnet generator were connected in parallel. Separate controllers were incorporated to regulate the DC bus voltage before feeding it to a pulse width modulation (PWM) inverter. Thus more number of power electronic interfaces is required for these hybrid grid-connected generator schemes. Subsequently, a grid-connected hybrid

Faculty of Electrical and Electronics Engineering, Saranathan College of Engineering, Tiruchirappalli, India, ** Faculty of Electrical and Electronics Engineering, National Institute of Technology, Tiruchirappalli, 620015 India, daniel@nitt.edu

ISSN 1335-3632

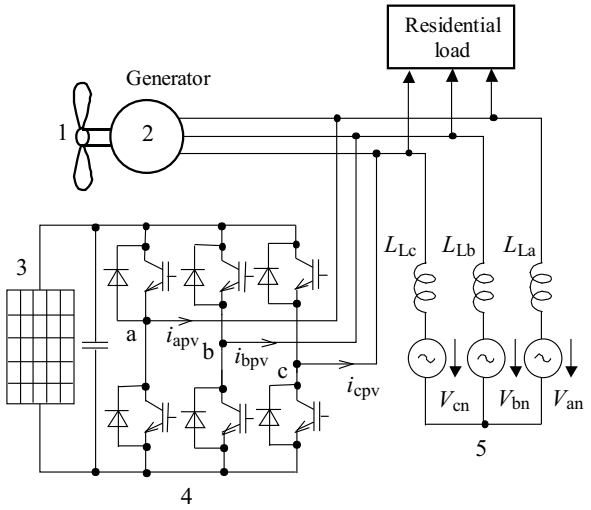

Fig. 1. Block schematic of grid connected hybrid scheme: 1 – Wind turbine, 2 – Induction generator, 3 – PV Array, 4 – Three-phase VSI, 5 – Grid

wind-PV scheme with AC-DC thyristor converter, a DC-AC thyristor inverter and an energy storage controlled by PLC containing a fuzzy logic module has been proposed [10]. Similarly, steady state performance of hybrid system based on PV and wind with battery storage connected to grid is investigated by [11]. In this scheme also, two stage conversions for grid integration is employed, since the wind turbine is coupled to a PM alternator. In order to overcome these difficulties in operating an induction generator in isolation in a otherwise grid connected scheme, a scheme integrating PV array with IG with or without battery storage is proposed in this paper. Earlier, a hybrid scheme employing PV array and induction generator supplying isolated load has been investigated [12-15]. However, the operation of the scheme in a non-autonomous grid connected mode requires a different control strategy for the inverter and this has been attempted in this paper. However, the scheme proposed in this paper has only an inverter for integrating the hybrid scheme with the utility network as compared to the earlier grid-connected hybrid schemes. Further, investigations on grid-connected hybrid wind-driven IG and PV scheme have not taken up so far and one such scheme is investigated in this paper.

2 DESCRIPTION OF THE SCHEME

The block schematic of the proposed scheme is shown in Fig. 1, where the PV array voltage is fed to a three-phase, six step Current-Controlled Voltage Source Inverter(CC-VSI). This CC-VSI is connected to the grid through an inductor. The controller for the inverter varies the inverter current to follow a reference current. The wind-driven induction generator is integrated with the grid when the wind-speed is greater than cut-in wind speed. The three-phase currents of the inverter are detected and compared with the corresponding phase-current references individually. The resulting current errors are directly used to generate the desired firing pulses for the inverter through an Average Current Mode Controller (ACMC). This is a current control technique that has fast response time and is capable of supporting wide range of power circuit topologies. The wind and PV generators can individually supply power to the grid and the control of the inverter meets the reactive power requirement of the induction generator. It should be noted that in the absence of the grid, the proposed scheme can supply power to a consumer by altering the current control of the inverter to simple SPWM operation. In such operation a three-phase fixed amplitude, fixed frequency supply obtained from the simple SPWM inverter forms the local grid to which the IG is kept integrated.

2.1 Development of the controller for the inverter

The block schematic of three phase current control VSI for the (phase A) is shown in Fig. 2. The inverter currents of other two phases are also detected and similarly compared with the corresponding phase current references.

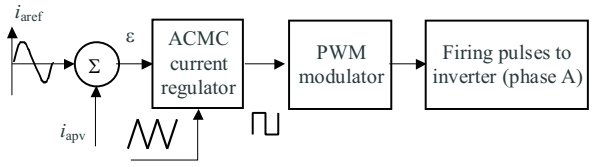

Fig. 2. representation PWM current controlled VSI (phase A)

At the first stage, the inverter output current is compared with a reference to produce error current signal ε. The ACMC takes this error current ε, as an input and it produces an average current error signal which is compared with a triangular waveform. The output of this comparator gives the required pulse width modulated signal for the inverter. Thus by varying the gating pulses applied to the CC-VSI the inverter current is made to follow the reference current value. The schematic representation of an integrator employed in the ACMC controller is indicated in Fig. 3.

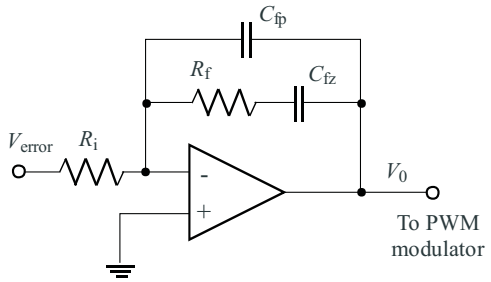

Fig. 3. Integrator circuit for VSI

The ACMC uses an integrating filter to produce an average current error signal and the transfer function of the integrator circuit is given in (1)

$$\frac{V_o}{V_{error}} = \frac{sR_fC_{fz}+1}{sR_i(sR_fC_{fp}C_{fz}+C_{fp}+C_{fz})} \tag{1}$$

where $V_{error} = V_{ref} - V_{inv}$ and V_0 is the output voltage of the ACMC. The filter component values are taken as given in [16]. The transfer function of the ACMC controller is given in (2).

$$\frac{V_o}{V_{error}} = \frac{(s+6250)}{1.3\times10^{-6}s(s+62795)}\,. \tag{2}$$

The integrated error signal is given to a PWM generator for generating firing pulses of the inverter.

3 MODELING AND ANALYSIS OF THE SCHEME

The synchronously rotating reference frame equivalent circuit of the induction machine with stepped stator voltages caused by the inverter operation is well established and is available in [17-18]. Nevertheless, in order to represent the proposed hybrid scheme in the synchronously rotating reference frame, the equivalent circuit of the induction generator is extended to include the current controlled VSI fed by PV array and the grid. The q axis and d axis equivalent circuit, of the hybrid system thus obtained is shown in Fig. 4 (a) and (b) respectively.

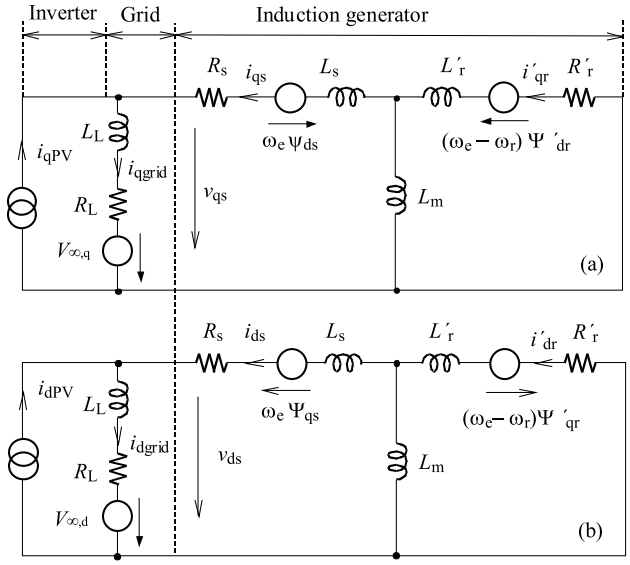

Fig. 4. $d-q$ axes model of the proposed system: (a) – axis equivalent circuit of the proposed system, where $\Psi_{ds} = L_s i_{ds} + L_m(i_{ds} + i'_{dr})$ and $\Psi'_{dr} = L_r i'_{dr} + L_m(i_{ds} + i'_{dr})$, (b) – axis equivalent circuit of the proposed system, where $\Psi_{qs} = L_s i_{qs} + L_m(i_{qs} + i'_{qr})$ and $\Psi'_{qr} = L_r i'_{qr} + L_m(i_{qs} + i'_{qr})$,

The equations of the induction machine in the time domain can be written as in [19]

$$\begin{bmatrix} v_{qs} & v_{ds} & 0 & 0 \end{bmatrix}^\top = \begin{bmatrix} R_s + L_s p & \omega_e L_s & L_m p & \omega_e L_m \\ -\omega_e L_s & R_s + L_s p & -\omega_e L_m & L_m p \\ L_m p & (\omega_e-\omega_r)L_m & R_r + L'_r p & (\omega_e-\omega_r)L'_r \\ -(\omega_e-\omega_r)L_m & L_m p & -(\omega_e-\omega_r)L'_r & R_r + L'_r p \end{bmatrix} \times \begin{bmatrix} i_{qs} & i_{ds} & i'_{qr} & i'_{dr} \end{bmatrix}^\top. \tag{3}$$

where p is simply an abbreviation of d/dt operator. The mechanical system is represented by equations (4) and (5)

$$\frac{\mathrm{d}}{\mathrm{d}t}\omega_r = \frac{1}{2H}(T_e - F\omega_r - T_m)\,, \tag{4}$$

$$T_e = -\Big(\frac{3}{2}\Big)\frac{P}{2}L_m(i_{qs}i'_{dr} - i_{ds}i'_{qr}) \tag{5}$$

where T_e is the electromagnetic torque, T_m is the mechanical shaft torque and P is the number of poles.

The machine voltages can be related with the grid voltage [20] as

$$v_{qs} = \sqrt{2}V_\infty\cos(\theta_{ef}(0)) + R_L i_{q\,grid} + L_L\frac{\mathrm{d}}{\mathrm{d}t}(i_{q\,grid}) + \omega_e L_L i_{d\,grid}, \tag{6}$$

$$v_{ds} = \sqrt{2}V_\infty\sin(\theta_{ef}(0)) + R_L i_{d\,grid} + L_L\frac{\mathrm{d}}{\mathrm{d}t}(i_{q\,grid}) + \omega_e L_L i_{q\,grid} \tag{7}$$

where R_L and L_L are equivalent resistance and inductance of the transmission line and V_∞ is the rms value of the grid voltage and $\theta_{ef}(0)$ is its phase with respect to q-axis.

The output of PV array is connected to CC-VSI and is integrated to the grid and the equivalent inverter currents controlled by PV array is as follows

$$i_{q\,PV} = \frac{2}{3}\Big(i_{a\,PV}\cos(\omega_e t) + i_{b\,PV}\cos\big(\omega_e t - \frac{2\pi}{3}\big) + i_{c\,PV}\cos\big(\omega_e t + \frac{2\pi}{3}\big)\Big), \tag{8}$$

$$i_{d\,PV} = \frac{2}{3}\Big(i_{a\,PV}\sin(\omega_e t) + i_{b\,PV}\sin\big(\omega_e t - \frac{2\pi}{3}\big) + i_{c\,PV}\sin\big(\omega_e t + \frac{2\pi}{3}\big)\Big). \tag{9}$$

Equations (3)–(9) has been utilized to study the dynamic behavior of the proposed system.

3.2 PV array model

The classical equation of a PV cell is quite well established and it describes the relationship between current I and voltage V of the cell as [21]

$$I_p = I_L - I_0\Big[\exp\Big(\frac{V_{pv}+R_{Se}I_{pv}}{V_T}\Big) - 1\Big] - \frac{V_{pv}+R_{Se}I_{pv}}{R_{sh}} \tag{10}$$

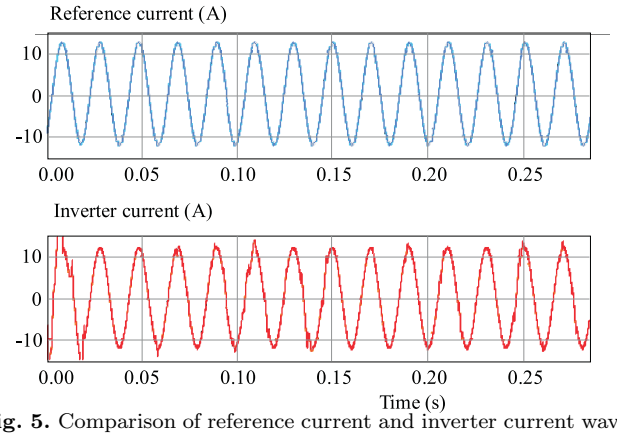

Fig. 5. Comparison of reference current and inverter current waveforms

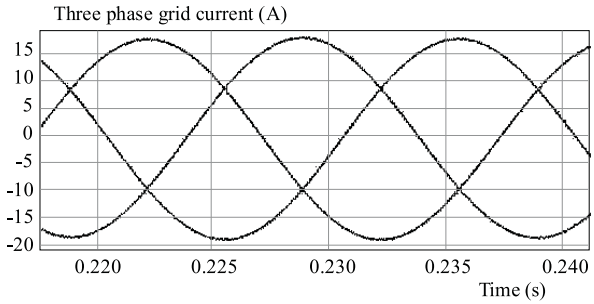

Fig. 6. Simulated three phase grid current waveform (0.05 s/div; 5A/div)

Neglecting the current in the shunt resistance ($I_{R\,sh} \cong 0$), (10) can be written as

$$I_p = I_L - I_0\Big[\exp\frac{V_{pv} + R_{Se}I_{pv}}{V_T} - 1\Big] \tag{11}$$

and assuming $\exp\Big(\frac{V_{pv}+R_{Se}I_{pv}}{V_T}\Big) \gg 1$, $I_L = I_{SC}$ and $I_0/I_{SC} \cong 10^{-9}$. Then (11) can be written as [22]

$$I_{pv} = I_{SC} - I_d \tag{12}$$

where

$$I_d \cong 10^{-9} I_{sc} \exp\Big(\frac{20.7}{V_{0c}}\big(V_{pv} + I_{pv}R_{sc}\big)\Big) \quad \because \ \big(V|_{I_{pv}=0} = V_{0c}\big)\,. \tag{13}$$

Equation (12) leads to the classical equivalent circuit with a constant current source in parallel with a diode. It is not possible to implement the classical equivalent circuit directly in the circuit simulation packages as a PV model, because the diode current I_d has to change as per the load variations and as a function of I_{SC} and V_{0c}. Thus the required variation in I_d is difficult to achieve through the accessible diode models of the available simulation platforms. As a result, the required V–I characteristic of a PV cell is not possible to be generated by a schematic of a classical equivalent circuit of a PV cell in circuit simulation software. Nevertheless, if the classical equivalent circuit is modified by replacing the diode by a controlled current source I_d, this modified circuit can be directly implemented as a PV model in circuit simulation software for simulating the proposed configuration.

3.3 Variation of model parameters with temperature and irradiation [23]

As a matter of fact, the short-circuit current of the PV array $I_{SC}(Q,T)$ at given irradiation Q and temperature T is strongly dependant on Q than on T and is given as

$$I_{sc}(Q,T) \cong I_{sc}Q(1 + \alpha\,\Delta T)\,. \tag{14}$$

On the other hand, $V_{OC}(Q,T)$ is a logarithmic function of Q and decreases with T and is given in (15)

$$V_{oc}(Q,T) \cong V_{oc}(1 - \gamma\,\Delta T)\ln(l + \beta\,\Delta Q)\,. \tag{15}$$

Further, the peak power $P_m(Q,T)$ is found by assuming that the form of the V–I characteristic remains the same with variation in Q and T and is given as

$$P_m(Q,T) \cong P_m\frac{I_{sc}(Q,T)V_{oc}(Q,T)}{V_{oc}I_{sc}}\,. \tag{16}$$

Since, at $I_{pv} = I_m$, $\delta V_{pv}/\delta I_{pv} = P_m/I_m^2$, from (1) $R_{se}(Q,T)$ and $I_m(Q,T)$ are obtained as follows

$$R_{se}(Q,T) \cong \frac{P_m(Q,T)}{I_m^2(Q,T)} - \frac{V_{oc}(Q,T)}{20.7[I_{sc}(Q,T) - I_m(Q,T)]}\,, \tag{17}$$

$$I_m(Q,T)\Big[1 + \frac{1}{20.7}\Big(\frac{I_m(Q,T)}{I_{sc}(Q,T) - I_m(Q,T)} + \ln\frac{I_{sc}(Q,T) - I_m(Q,T)}{I_{sc}(Q,T)}\Big)\Big] = \frac{2P_m(Q,T)}{V_{oc}}\,. \tag{18}$$

The variation of parameters of the developed PV model with respect to temperature and irradiation can be obtained from (14)–(18) using the basic parameters of V_{0c}, I_{SC}, and P_m at standard temperature and irradiation as supplied by the manufacturers and assuming typical values of α, β, γ as 0.0025 per °C, 0.5 per *Sun*, 0.00288 V per °C correspondingly.

4 ANALYSIS OF THE SCHEME

The proposed hybrid grid connected scheme is simulated in Simpower of MATLAB. The PV array is made up of 40 panels connected in series with four such strings in parallel. Each panel is rated 80 W, 22 V and 4.7 A. The array is thus capable of supplying 9.8 $\mathrm{kW_p}$. The wind-driven squirrel cage induction machine is rated 7.5 kW, 400 V, Y connected, 4 poles, 1500 rpm. The output of the PV array is inverted by means of a three-phase 6-pulse IGBT inverter and the inverter feeds the grid at a phase-voltage of 230V. The switching frequency of the inverter is taken as 10 kHz. The measured current at each phase

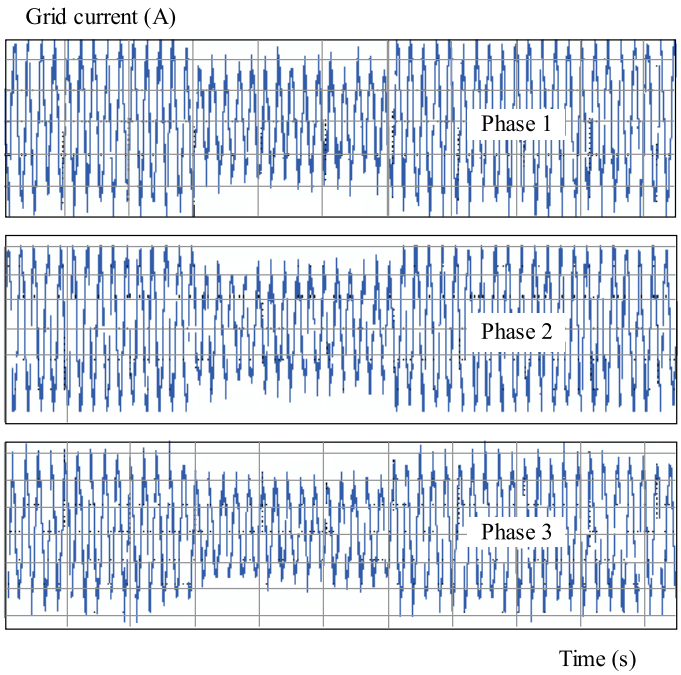

Fig. 7. Three-phase grid connected waveforms subjected to varying reference currents at $t = 0.3$ s and at $t = 0.6$ s (0.1 s/div; 5 A/div)

of the inverter is compared with the set reference current and the decoupled current error signal is put through a transfer function of an average current mode regulator realized using OP-AMPs. The pole, zero and gain of the current controller are designed as in Eq. (2). The output of the ACMC controller is given to the PWM modulator to generate firing pulses for VSI. The parameter of the PV array are obtained for different temperature and irradiation from the equations given in section 3.3 and are employed to analyze the operation of the scheme for varying irradiations and wind speed. The inverter current obtained from the designed current controller and the reference currents have been compared and indicated in Fig. 5. As evident from Fig. 5, the inverter current closely follows the reference current with the designed ACMC controller.

The injected grid current for irradiation of $0.8\,\mathrm{kWm^{-2}}$ and shaft torque of 40 N-m. is shown in Fig. 6. The entire CC-VSI fed by PV array is subjected to rapid variations in the reference current to the current controller to ascertain the ability of the controller to adapt to varying irradiation conditions. The simulated dynamic response of the controller as shown in Fig. 7, demonstrates the ability of the controller to rapidly switch to the varying references instantaneously.

the real and reactive power flow to the grid for varying irradiation and torque is observed and recorded for varying amplitude and phase angle θ of the inverter current. The feasibility of the hybrid generator to inject current to the grid at different power factors is illustrated by means of phasor diagrams.

Case i: When the wind speed increases, the shaft torque of induction generator increases and reactive power consumed by the induction generator increases. However, in the proposed scheme, when there is sufficient irradiation and the phase angle θ of the reference current I_{inv} is made greater than ϕ, (where ϕ is the angle between the induction generator current I_{ig} and the grid voltage V_{grid}), then leading current is injected into the grid. In this case, the PV array meets the reactive power requirements of the induction generator and supplies excess reactive power to the grid for any

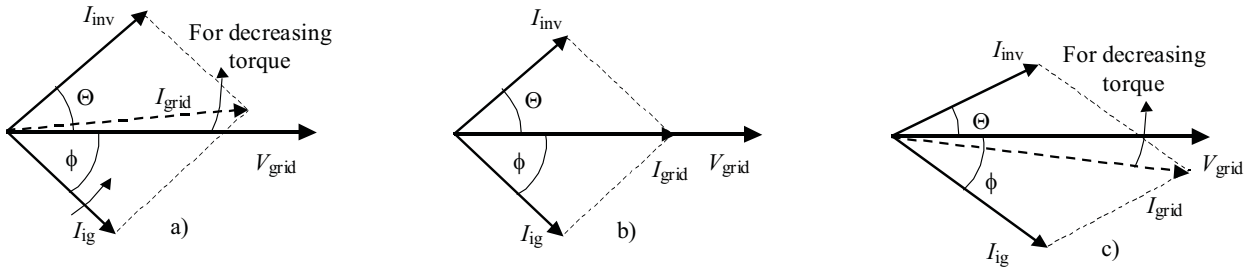

Fig. 8. Phasor representation of grid connected operation: (a) – Leading power factor operation, (b) – unity power factor operation, (c) – Lagging power factor operation

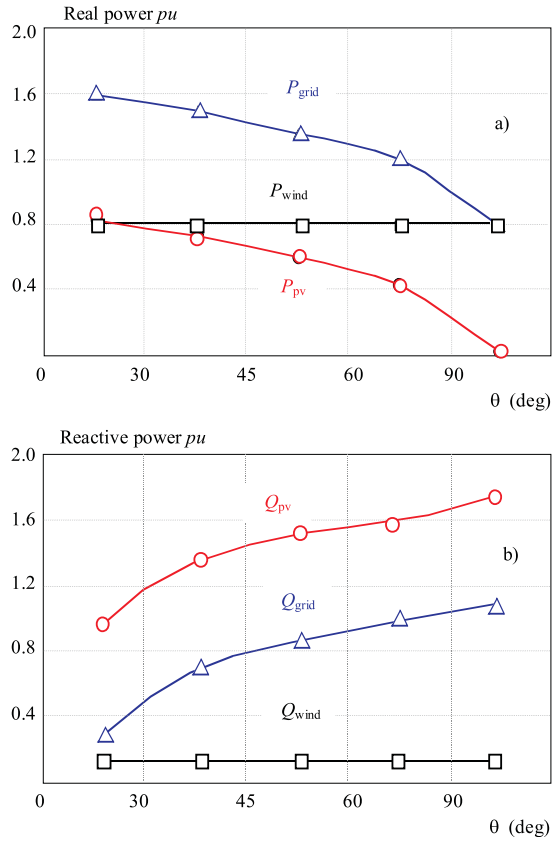

Fig. 9. Power flow variations for maximum irradiation and torque: (a) – Real power flow variation, (b) – Reactive power flow variation

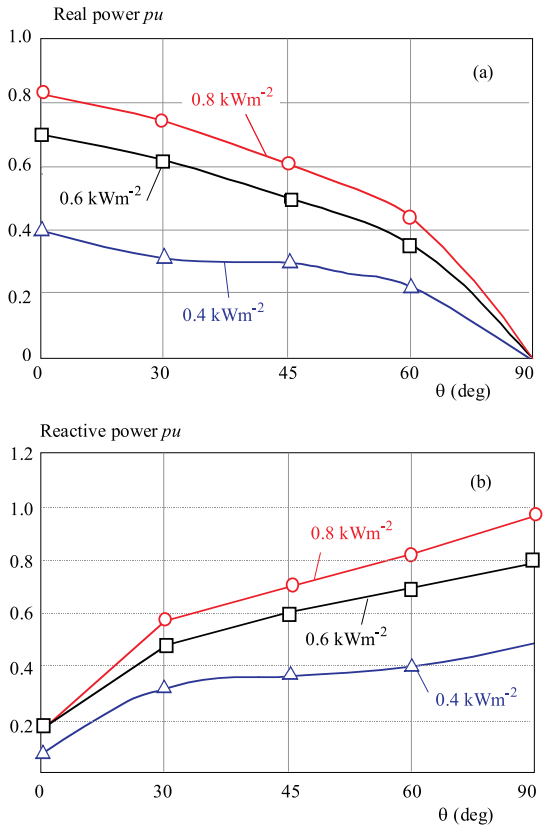

Fig. 10. Power flow variations for varying irradiation: (a) – Real power flow variation, (b) – Reactive power flow variation

wind speed and the phasor representation is indicated in Fig. 8(a).

Case ii: By appropriately varying the phase angle θ of reference current such that it is same as ϕ, it is possible to deliver current with unity power factor to the grid as indicated in Fig. 8(b). This condition has also been ascertained for varying torque and irradiation conditions.

Case iii: Even when the irradiation and wind speed is high, it is observed that if the reference phase lead is less than ϕ, then grid current lags the grid voltage as illustrated in Fig. 8(c). The leading VARs supplied by the PV array is decreased and consequently the reactive power requirements of the induction generator are met partly by the grid and PV.

4.1 Power flow variations for maximum irradiation and torque

The grid connected scheme is simulated and tested under the condition of maximum irradiation ($0.8\,\mathrm{kWm^{-2}}$) and wind speed (torque of 40 N-m). The maximum irradiation under standard conditions is $1\,\mathrm{kWm^{-2}}$ and the maximum torque is computed from the machine rating. The real power supplied by the PV array P_{pv} and the wind-generator P_{wind} to the grid is presented in Fig. 9(a). The real power fed to the grid P_{grid} and the residential load P_R is supplied by PV and wind generators. Hence,

$$P_{Pv} + P_{wind} = P_{grid} + P_R\,, \tag{19}$$

$$3V_{grid}I_{PV}\cos\theta + 3V_{grid}I_{ig}\cos\phi = P_{grid} + P_R\,. \tag{20}$$

The reactive power flow variation for the same condition of torque is indicated in Eq. (12) and the simulation results in Fig. 9(b)

$$3V_{grid}I_{PV}\sin\theta + 3V_{grid}I_{ig}\sin\phi \leftrightarrow Q_{grid} \pm Q_R\,. \tag{21}$$

As the phase lead advances, the reactive power requirement of the induction generator Q_{wind} and the residential load Q_R is completely supplied by PV array Q_{pv} and excess reactive power is fed to the grid Q_{grid} as evident in Fig. 9(b).

4.2 Variation in real and reactive power flow of PV array

The real power supplied by the PV array for varying irradiation and a shaft torque of 40 N-m. is simulated for varying phase angle and amplitude of reference current of the controller. Maximum real power is supplied by the PV array when the power factor and irradiation is maximum and reduces as the power factor of operation is reduced as indicated in Fig. 10(a). Similarly the reactive power flow for varying irradiation is plotted in Fig. 10(b).

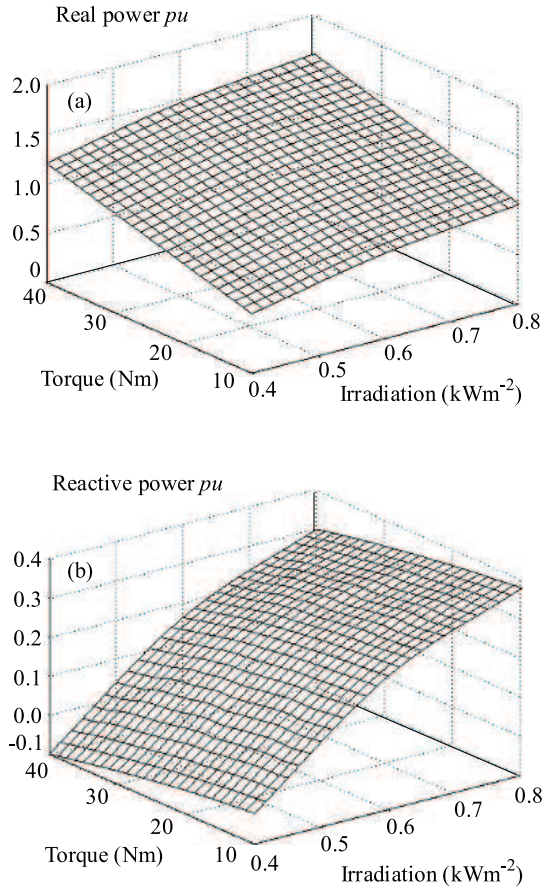

Fig. 11. Power flow variations in the grid for varying torque and irradiation conditions: (a) – Real power flow variations for $\theta = 0°$, (b) – Reactive power flow variations for $\theta = 90°$

4.3 Real and Reactive power flow variations of grid for varying irradiation and torque

A three dimensional plot to study the variation of real power fed when the hybrid scheme is operated at different power factors is shown in Fig. 11a. The reduction in the real power from the array at low power factor operation can be compensated by the induction generator. This is true for any wind speed above the cut-in speed, but irradiation must be greater than the threshold value ($0.4\,\mathrm{kWm^{-2}}$). The reactive power flow variation for $\theta = 90°$ for varying conditions of torque and irradiation is indicated in Fig. 11b. The grid supplies the reactive power when the irradiation and wind speed are minimum and when the irradiation increases, the PV array meets the reactive power requirement of the induction generator and excess reactive power is supplied to the grid.

5 CONCLUSION

A hybrid dispersed generator employing a PV array and wind driven induction generator has been investigated. The hybrid generator is integrated to a three phase grid using a simple three-phase inverter. The PV array in the scheme is controlled to act as VAR compensator for the wind-driven induction generator and also as a source of real power to the grid. The *dq* axis model of the grid connected hybrid scheme has been developed and exhaustive simulations have brought out the capability of the controller to deliver currents at varying power factor. The operation of the hybrid generator to supply real and reactive power under varying torque and irradiation has been simulated and the results presented. Further, the range of irradiation and wind speeds for which reactive power could be fed into the grid is identified for a given rating of the hybrid generator. Furthermore, the real and reactive power limits for varying phase angle of the reference current of the controller for a given irradiation and windspeed are identified. The Simpower model can be utilized to investigate the operation of a hybrid generator of any rating.

6 NOMENCLATURE

I_{grid}	RMS value of grid current (A)
I_{ig}	RMS value of Induction generator current (A)
I_{PV}	RMS value of Inverter current (A)
R_s, R'_r, R_L	resistances of stator, rotor (referred to the stator winding) and transmission line (Ω)
I_s, L'_r	per phase inductances of stator, rotor (H)
L_L	Equivalent reactance of transmission line
L_m	per phase magnetizing inductance (H)
Ψ_{ds}	d-axis stator flux linkage (Wb)
Ψ_{qs}	q-axis stator flux linkage (Wb)
Ψ'_{dr}	d-axis rotor flux linkage (refererd to stator winding) (Wb)
Ψ'_{qr}	q-axis rotor flux linkage (refererd to stator winding) (Wb)
V_∞	RMS value of grid voltage (V)
i_q, i_d	quadrature and direct-axis machine currents (A)
v_q, v_d	quadrature and direct-axis machine voltages (V)
H	inertia constant of rotor (s)
ω_e, ω_r	angular speeds of reference-frame and rotor (1/sec)
P_{pv}, P_{wind}	Real power delivered by PV array and IG *pu*
P_{grid}	Real power fed to the grid *pu*
P_R	Real power fed to the residential load *pu*
Q_{PV}	Reactive power supplied by PV array *pu*
Q_{wind}	Reactive power of Induction generator *pu*
Q_{grid}	Grid reactive power fed to the grid *pu*
Q_R	Reactive power consumed by the load *pu*

References

[1] SLOOTWEG, J. G.—KLING, W. L.: Impacts of Distributed Generation on Power System Transient Stability, IEEE power Engineering society summer meeting 2002; 2:863–867.

[2] CHANDHAKET, S.—KONISHI, Y.—OGURA, K.—NAKAOKA, M.: Utility AC Interfaced Soft-Switching Sinewave PWM Power Conditioner with Two-Switch Flyback High-Frequency Transformer, IEE Proc. Electr. Power Appl. **151** No. 5 (2004), 526–533.

[3] CHOWDHURY, B. H.—SAWAB, A. W.: Evaluating the Value of Distributed Photovoltaic Generations in Radial Distribution Systems, IEEE Transactions on Energy Conversions **11** **595–600** (1996).

[4] CHANG, L.—DIDUCH, C.: Issues of Interconnecting Distributed Power Generators with Electric Grids, Canadian Conference on Electrical and Computer Engineering **1** (2003), 675–678.

[5] BANSAL, R. C.—BHATTI, T. S.—KOTHARI, D. P.: A bibliographical Survey on Induction Generators for Application of Non-Conventional Energy System, IEEE Transactions on Energy Conversion **18** (2003), 433–439.

[6] CHAN, T. F.: Capacitance Requirement of Self-Excited Induction Generators, IEEE Transaction on Energy Conversion **8** (1993), 304–311.

[7] MARRA, E. G.—POMILIO, J. A.: Induction-Generator Based System Providing Regulated Voltage with Constant Frequency, IEEE Trans. Industrial .Electronics **47** (2000), 908–914.

[8] OJO, O.—DAVIDISON, I. E.: PWM-VSI Inverter Assisted Standalone Dual Stator Winding Induction Generator, IEEE Trans. Ind. Applications No. 6 (2000 36), 1604–1611.

[9] DAS, D.—ESMAILI, R.—XU, L.—NICHOLS, D.: An Optimal Design of a Grid Connected Hybrid Wind/Photovoltaic/Fuel Cell System for Distributed Energy Production, in Proc. 2005 IEEE Industrial Electronics Society Conf. 2499–2504.

[10] WANG, L.—LIU, K. H.: Transient Performance and Stability Analysis of a Hybrid Grid-Connected Wind/PV System, in Proc. 2004 IEEE Power Systems Conf. pp. 795–801.

[11] GIRAUD, F.—SALAMEH, Z. M.: Steady-State Performance of a Grid-Connected Rooftop Hybrid Wind-Photovoltaic Power System with Battery Storage, IEEE Transactions on Energy Conversion **16** (2006), 1–7.

[12] DANIEL, S. A.—GOUNDEN, N. A.: A Novel Hybrid Isolated Generating System Based on PV Fed Inverter-Assisted Wind-Driven Induction Generators, IEEE Transactions on Energy Conversions **19** No. 2 (2004), 595–600.

[13] ARUTCHELVI, M.—DANIEL, S. A.: Voltage Control of an Autonomous Hybrid Generation Scheme Base on PV Array and Wind-Driven Induction Generators, Electric Power Components and Systems **34** No. 7 (2006), 759–773.

[14] ARUTCHELVI, M.—DANIEL, S. A.: Composite Controller for a Hybrid Power Plant Based on PV Array Fed Wind-Driven Induction Generator with Battery Storage, International Journal of Energy Research **31** No. 5 (2007), 515–524.

[15] BADEJANI, M. M.—MASOUM, M. A. S.—KALANTAR, M.: Optimal Design and Modeling of Stand-Alone Hybrid PV-Wind Systems, Universities Power Engineering Conference, 2007. AUPEC 2007. Australasian, pp. 1–6, 9-12 Dec 2007.

[16] Baker,D.M.;Agelidis,V.G.;Nayar,C.V.: Simulation of a Full-Bridge Current Controlled Grid-Connected Inverter System, www.ceanet.com.au\kb\papers\simulation_of_a_full.htm.

[17] KRAUSE, P. C.: Analysis of Electric Machinery, McGraw-Hill Book Co., 1987.

[18] BOSE, K.: Power Electronics and AC Drives, Prentice-Hall, Englewood Cliffs, New Jersey, 1986.

[19] WANG, L.—LEE, C. H.: A Novel Analysis on the Performance of an Isolated Self-Excited Induction Generator, IEEE Trans. on EC **12** No. 2 (June 1997).

[20] WANG, L.—YANG, Y. F.—KUO, S. C.: Analysis of Grid-Connected Induction Generators under Three-Phase Balanced Conditions, Power engineering society winter meeting 2002, 1: 413–417.

[21] BISHOP, J. W.: Computer Simulation of the Effects of Electrical Mismatches in Photovoltaic Cell Interconnection Circuits, Solar Cells **25** (1988), 73–89.

[22] KOU, Q.—KLEIN, S. A.—BECKMAN, W. A.: A Method for Estimating the Long-Term Performance of Direct-Coupled PV Pumping Systems, Solar Energy **64** (1998), 33–40.

[23] SINGER, S.—ROZENSHTEIN, B.—SURAZI, S.: Characterization of PV Array Output using a Small Number of Measured Parameters, Solar Energy **32** (1984), 603–607.

Received 27 January 2009

Meenakshisundaram Arutchelvi was born in Tiruchirappalli, India in 1967. She received her BE degree in Electrical Engineering from Vishveshvaraiah college of Engineering, Bangalore in 1990 and ME in Power systems in 1994 and PhD in Electrical Engineering from National Institute of Technology, Tiruchirappalli in 2007. Her main research interest is in dispersed power generators based on PV and wind power generators and power electronics. Currently, she is a Professor of Electrical Engineering at Saranathan College of Engineering, Tiruchirappalli, India.

Samuel Arul Daniel was born in Tiruchirappalli, India, 1967. He received his BE degree from Government College of Technology in 1988 and ME in Power Systems and PhD in Electrical Engineering from National Institute of Technology, Tiruchirappalli in 1991 and 2003 respectively. He was a British Council study fellow under Prof. N. Jenkins at UMIST, Manchester during 1997. Currently, he is working as Asst. Professor in the Department of Electrical and Electronics, National Institute of Technology, Tiruchirappalli, India. His areas of interest are micro-grids, distributed generators and renewable resources.